OFFICE OF NAVAL RESEARCH

Grant: N00014-95-WR-20027

PR: Number 96PRO-3804

Technical Report No. 11

X-ray Absorption and Magnetic Resonance Spectroscopic Studies of LixV6O13

by

P. E. Stallworth*, S. Kostov**, M. L. denBoer**, S. G. Greenbaum** and
C. Lampe-Onnerud***

Prepared for Publication in
Journal of Applied Physics

*United States Naval Academy
Physics Department
Annapolis, MD 21402

**Physics Department
Hunter College of CUNY
New York, NY 10021 USA

***Quantum Energy Technologies, Inc.
Cambridge, MA 02142

June 27, 1996

REPORT DOCUMENTATION PAGE

Form Approved
OMB No. 0704-0188

1. AGENCY USE ONLY (Leave blank)	2. REPORT DATE	3. REPORT TYPE AND DATES COVERED
	June 27, 1996	Technical Report 6/1/95 - 5/31/96

4. TITLE AND SUBTITLE
X-ray Absorption and Magnetic Resonance Spectroscopic Studies of LixV6O13

5. FUNDING NUMBERS
Grant:
N00014-95-WR-20027
PR Number:
96PRO-3804
Robert J. Nowak

6. AUTHOR(S)
P. E. Stallworth, S. Kostov, M. L. denBoer,
S. G. Greenbaum and C. Lampe-Onnerud

7. PERFORMING ORGANIZATION NAME(S) AND ADDRESS(ES)
United States Naval Academy
Physics Department
Annapolis, MD 21402

8. PERFORMING ORGANIZATION REPORT NUMBER
Technical Report #11

9. SPONSORING/MONITORING AGENCY NAME(S) AND ADDRESS(ES)
Office of Naval Research
Chemistry Division
800 North Quincy Street
Arlington, VA 22217-5660

10. SPONSORING/MONITORING AGENCY REPORT NUMBER

11. SUPPLEMENTARY NOTES
Prepared for Publication in Journal of Applied Physics

12a. DISTRIBUTION/AVAILABILITY STATEMENT
Reproduction in whole or in part is permitted for any purpose of the United States Government. This document has been approved for public release and sale; its distribution is unlimited.

12b. DISTRIBUTION CODE

13. ABSTRACT *(Maximum 200 words)*
Polycrystalline LixV6O13 samples, 0.5<x<6, were prepared by chemical intercalation in n-butyl lithium and investigated by various spectroscopic techniques, including x-ray absorption, electron paramagnetic resonance (EPR), and 7Li solid state nuclear magnetic resonance (NMR). The EPR results, which are sensitive to the total V+4 concentration, are consistent with the expectation that the formal oxidation state of vanadium decreases monotonically with the addition of Li. This is confirmed by near-edge x-ray absorption fine structure spectra at the vanadium K-edge. The extended x-ray absorption fine structure shows that the local symmetry of the vanadium sites, as determined by the intensity of the first V-O peak in the radial distribution function, decreases with increasing x from 0<x<1 and then increases with increasing x from 1<x<5. However, structural correlations beyond the nearest neighbor atoms rapidly decrease with increasing Li content above x=1.5. A modest lattice expansion due to intercalated Li is inferred from the observed increase in the V-O radial distribution peak position, from 1.93 Angstroms at x=0 (in agreement with x-ray diffraction results) to 2.02 Angstroms at x=5. Variable temperature 7Li NMR linewidth and spin-lattice relaxation measurements demonstrate that, at all concentrations studied (0.5<x<6) the Li ions are relatively immobile, even at 200 deg. Centigrade. At low Li concentrations (up to x=1.5) the Li ions tend to reside near V+5 sites rather than paramagnetic V+4 or V+3 sites.

14. SUBJECT TERMS
EXAFS, NMR, cathode material

15. NUMBER OF PAGES

16. PRICE CODE

17. SECURITY CLASSIFICATION OF REPORT	18. SECURITY CLASSIFICATION OF THIS PAGE	19. SECURITY CLASSIFICATION OF ABSTRACT	20. LIMITATION OF ABSTRACT
UNCLASSIFIED	UNCLASSIFIED	UNCLASSFIED	

X-ray Absorption and Magnetic Resonance Spectroscopic Studies of $Li_xV_6O_{13}$

P. E. Stallworth*, S. Kostov+, M. L. denBoer+, S. G. Greenbaum+ and C. Lampe-Onnerud**

* Physics Department, U.S. Naval Academy, Annapolis, MD 21402.

+ Physics Department, Hunter College of CUNY, New York, NY 10021.

** Chemistry Department, Massachusetts Institute of Technology, Cambridge, MA 02139;

present address: Quantum Energy Technologies, Inc. 238 Main St., Cambridge, MA 02142.

ABSTRACT

Polycrystalline $Li_xV_6O_{13}$ samples, $0.5 \leq x \leq 6$, were prepared by chemical intercalation in n-butyl lithium and investigated spectroscopically by x-ray absorption, electron paramagnetic resonance (EPR), and ^7Li solid state nuclear magnetic resonance (NMR). The EPR results, which are sensitive to the total V^{+4} concentration, are consistent with the expectation that the formal oxidation state of V decreases monotonically with the addition of Li. This is confirmed by near-edge x-ray absorption fine structure spectra at the vanadium K edge. The local symmetry of the V ions first decreases with increasing x from $0 \leq x \leq 1$ and then increases with increasing x from $1 < x \leq 5$, becoming increasingly octahedral. These changes are revealed by both the intensity of the first V-O peak in the radial distribution function and by the decrease in the x-ray absorption pre-edge peak intensity. However, structural correlations beyond the nearest neighbor atoms rapidly decrease with increasing Li content above $x = 1.5$, reflecting increased disorder. The observed increase in the first V-O distance implies a modest lattice expansion with intercalated Li, from 1.93 Å at $x = 0$ (in agreement with x-ray diffraction results) to 2.02 Å at $x = 5$. Variable temperature ^7Li NMR linewidth and spin-lattice relaxation measurements demonstrate that at all concentrations the Li ions are relatively immobile, even at 200 °C. At low Li concentrations ($x \leq 1.5$) the Li ions tend to reside nearer V^{+5} sites than paramagnetic V^{+4} or V^{+3} sites.

Introduction

Vanadium oxides have attracted considerable attention as possible cathodes in lithium batteries.[1] Several compounds, with mean vanadium oxidation states ranging from +5 in V_2O_5 to +4 in VO_2, have been investigated for cathode applications. V_6O_{13} has emerged as one of the most favorable candidates, as it has a high theoretical capacity. Important questions including the maximum Li uptake and the identification of specific stoichiometries have been addressed by several groups.[2],[3],[4],[5] Recent work by one of us has identified four different phases which form in chemically intercalated $Li_xV_6O_{13}$ as a function of *x*: $Li_{0.5}V_6O_{13}$, $Li_{1.5}V_6O_{13}$, $Li_3V_6O_{13}$, and $Li_6V_6O_{13}$.[2],[6] Both chemically and electrochemically intercalated samples were tested and it was shown that both the battery performance and the intercalation process varied greatly with phase purity.

We have used complementary spectroscopic methods to probe both the structural and electronic environment of both the transition metal and the lithium cation. These methods are: near-edge x-ray absorption fine structure (NEXAFS), extended x-ray absorption fine structure (EXAFS), electron paramagnetic resonance (EPR), and solid state ^{7}Li nuclear magnetic resonance (NMR). Previous EPR[7] and ^{7}Li NMR[8] studies of V_2O_5 and x-ray absorption studies of $Li_{1+x}V_3O_8$[9] have been reported.

Experiment

$Li_xV_6O_{13}$ samples with $x = 0$, 0.5, 1, 1.5, 2, 3, 4, 5, and 6 were prepared from phase-pure V_6O_{13} made by thermal decomposition as described in detail in Ref. [2]. Chemical intercalation was performed in sealed 25 ml glass bottles sealed with a teflon-silicon septum, through which n-

butyl lithium (Merck, 1.6 M in hexane) was added with a Hamilton syringe (1000 ± 0.005 ml). After proceeding for 20 h, the reaction was stopped by evaporating the hexane with flowing argon. Samples were made ready for spectroscopic measurement under controlled conditions in a dry glove box to prevent exposure to atmospheric water. For EPR and NMR, samples were sealed into quartz tubes. For x-ray absorption, for which quartz would absorb too strongly, they were sealed into paraffin and kapton tape.

Electron Paramagnetic Resonance

Electron paramagnetic resonance (EPR) measurements were performed at room temperature on an IBM/Bruker ER-220 X-band EPR spectrometer. EPR spectra were obtained in single field-sweep mode. Spectral intensities were corrected for effects due to varying receiver gain and/or microwave power on each sample.

X-ray Absorption

Near-edge x-ray absorption fine structure (NEXAFS) and extended x-ray absorption fine structure (EXAFS) measurements of the vanadium K edge were made at room temperature in transmission at beam line X-23B at the National Synchrotron Light Source at Brookhaven National Laboratory using a double Si(111) crystal monochromator. The energy resolution was typically ~1 eV, although smaller shifts could be detected by the use of a reference sample. As is customary, all spectra were normalized to the main edge jump.

Solid State NMR

NMR measurements were carried out at temperatures from -150 to 200 °C on a Chemagnetics CMX 300 spectrometer operating at a ^{7}Li resonance frequency of 116.99 MHz. Sample volumes were roughly 0.2 cm^3 and excellent signal-to-noise was obtained after

accumulating 200 to 400 transients. ^{7}Li lineshapes were obtained employing a single $\pi/2$ pulse (typically 3 μs width) sequence followed by acquisition of the free induction decay. Spin-lattice relaxation time (T_1) measurements were performed using either a saturation-recovery or an inversion-recovery pulse sequence.

Results and Discussion

EPR

X-band EPR spectra for $Li_xV_6O_{13}$ are shown in Fig.1(a) (x = 0, 0.5, 1.0, and 1.5) and Fig.1(b) (x = 2, 3, 4, 5, and 6). The nominal vanadium valence for x = 0 is +4.33, which is a superposition of the stable +4 and +5 states. However, since EPR is sensitive only to the paramagnetic +4 state, the integrated intensity will be proportional to the +4 concentration. If intercalation occurs, the neutral Li will become ionized and cause a reduction of the vanadium valence, i.e., more V^{+4}. This is evidently the case; Fig.1 shows the EPR signal steadily increases to its maximum value for x = 2, which corresponds to the highest V^{+4} concentration (nominally 100 %). By x = 2 the spectrum has also become very broad (width changes have of course no effect on the integrated intensity) due to strong magnetic dipole-dipole interactions. With the addition of Li beyond x = 2 the EPR signal decreases, as shown in Fig.1(b). Under the present experimental conditions (room temperature and 3 cm microwave wavelength), EPR is apparently not sensitive to the V^{+3} formed by the additional charge contributed by the Li. We attribute this to relatively large zero-field splittings and short relaxation times.[10] These EPR results thus confirm the expectation that the intercalation reaction proceeds smoothly, at least up to x = 5. However, preliminary ^{51}V NMR results have shown that some V^{+5} remains at all value of x;

further quantitative studies are in progress. We regard the slight increase in EPR signal at $x = 6$ as anomalous; a suitable explanation has not been found.

X-ray Absorption

1. Near-Edge (NEXAFS) Region

Fig.2(a) shows the overall vanadium K-edge spectra of $Li_xV_6O_{13}$ as a function of x. The main absorption edge appears at about 5475 eV. The "pre-edge" region before the main edge is shown on an expanded scale in Fig. 2(b). This pre-edge has been shown to be due to $s \rightarrow d$ transitions which, while dipole-forbidden, become allowed in non-octahedral symmetry as the V $3d$ states mix with the O p states.[11] Therefore the strength of this transition, which may be measured by integrating the area of the peak above background, is proportional to the deviation from local octahedral symmetry of the vanadium site.[12] It is evident from Fig. 2(b) that the transition strength first increases slightly with increasing x for $x < 1$ and then decreases rapidly for $x > 1.5$, except for $x = 6.0$, which we believe is anomalous, just as the previously mentioned EPR result. The structural changes these results imply are corroborated by EXAFS analysis and further discussed below.

The "white line" peak after the edge jump gives additional information about the chemical environment of the vanadium. The white line intensity is proportional to the number of $s \rightarrow p$ transitions, so it in effect probes unoccupied final states of p symmetry.[13] There may also be localized exciton levels occasioned by the screening of the core hole.[14] The white line peak is shown expanded in Fig.2(c) as a function of x. Clearly, this peak grows dramatically with

increasing Li concentration. At low Li concentrations, $x = 0$ to $x = 1$, i.e, high oxidation state values, the white line exhibits a possible ligand splitting effect.[15]

As shown in Fig. 2(a), the main absorption edge shifts monotonically to lower binding energy with increasing Li concentration. This shift attains its largest value of ~1 eV for $x = 6.0$. The shift is due to reduction of the formal valence of V, from 4.33 for $x = 0$, by the addition of electrons donated by Li. This additional negative charge reduces the effective binding energy of all the electrons at the V site and better screens the core hole produced in the x-ray absorption event. In a mixed-valent material like $Li_xV_6O_{13}$, the shift is an average over the V ions in each oxidation state. Consistent with the EPR results, this shift shows that the average V valence decreases uniformly with increasing x.

2. Extended Region (EXAFS)

The extended x-ray absorption fine structure (EXAFS) above the vanadium K edge gives valuable structural information about the local geometry around the V ions, including the distances from V to near neighbor atoms and the number of such atoms in each coordination shell. We have determined the local structure for the stoichiometric compound and measured deviations from that for the intercalated series.

To extract the EXAFS from the measured absorption spectrum, it is necessary to remove the relatively smooth background atomic absorption above the edge. The correct approximation of this background absorption has been widely discussed in the literature. We have used a procedure included in an analysis package, UWXAFS [16], which uses minimization of non-physical low-r peaks in the radial distribution as the primary criterion for the background

determination. This offers the additional advantage that the range in k space available for reliable EXAFS analysis may be extended to k values as low as 1.5Å, particularly helpful in disordered materials such as $Li_xV_6O_{13}$ in which the k range tends to be restricted. The signal was weighted by k^3 to compensate for attenuation with increasing k. The resulting oscillations were Fourier transformed to produce the radial distribution functions (RDF's) in Fig. 4(a). Peaks in this function correspond to interatomic spacings in the vicinity of the V.

We now describe the fitting of these measured features to calculated functions. V_6O_{13} has been studied with single crystal and powder x-ray diffraction methods. The structure is layered octahedral,[17] and lattice constants and interatomic distances have been reported.[18] We use this information to calculate an EXAFS spectrum, using the package FEFF 6.01 [19], to compare with the experimental data. The simple geometrical model used is shown in Fig. 3. There are three vanadium sites, V_1, V_2, and V_3, which are inequivalent due to the varying coordination with more distant octahedra and contribute equally to the spectrum, both theoretical and measured. The model does not take into account the monoclinic symmetry of the lattice, assuming instead for simplicity that each layer is composed of perfect octahedra placed on a rectangular grid and centered at the vanadium sites with oxygen atoms at the vertices. The assumption of perfect octahedra neglects the fact that in the actual structure the octahedra are distorted and there is a range of V-O distances from 1.64 to 2.28 Å. This simplification has little effect on the first shell calculations, but strongly distorts more distant shells with multiple paths. We therefore restricted the model cluster to 4 Å for each site. This restriction and, more importantly, the assumption of single oxygen distances, reduces the overall amplitude of the calculated spectrum by a factor ~5 due to the lack of interference damping of the reflected electron waves.

The theoretical spectrum thus generated was fitted to the experimental data in r space. The fitting routine, also part of the UWXAFS package, minimizes the least-squares difference between the amplitude of the theoretical RDF's and those obtained by Fourier transformation of the experimental data. Fitting in r space has the advantage that the amplitude function has a direct physical interpretation, as it is related directly to actual interatomic spacings. The best fit parameters are given in Table 2, and in Fig. 4(b) we compare the best fit single-shell functions to the experimental RDF for the stoichiometric compound. While these fits are not exact by standard statistical criteria, they are stable with respect to different types of background removal, weighting, and windowing and are therefore not merely local minima in parameter space, but have actual physical significance. In particular, the first shell vanadium-oxygen distances are in excellent agreement with the average crystallographic values, as shown in Table 1. This supports the simple model used and facilitates measurement of changes in the near-neighbor environment of the V.

We now consider the structural changes as a function of Li. Several distinct trends are apparent:

1. Fig. 4(a) shows the intensity and relative sharpness of the first peak, which corresponds to the V-O distance in the first octahedron, increase with x, reaching a maximum at $x = 5$ (once again, the $x = 6$ result we regard as anomalous). The quality of the fit also improves, as shown by way of example in Fig. 4(c) for $x = 5$. These observations imply that the range of V-O distances in the first shell is becoming smaller, i.e, these distances are all becoming the same, i.e., the local V-O octahedra are becoming less distorted. This is strong confirmation, by a completely independent measurement, of the conclusion implied by the decrease in the pre-edge

intensity with increasing x, discussed earlier. We plot these two observations, the changes in pre-edge intensity and in amplitude of the first RDF peak, in Fig. 5(a). The agreement between these measurements, at every value of x, is remarkable. Both indicate that there are several distinct regimes. For $x < 1$ there is a slight increase in the distortion from octahedral symmetry with increasing x, while from $x = 1$ to 3 there is a dramatic decrease in the octahedral distortion. Beyond $x = 3$ there is little change apart from the anomalous $x = 6$ sample.

2. Increasing disorder, as discussed below, makes quantitative estimates of the change in lattice size due to intercalation difficult and somewhat less meaningful. However, on the basis of the expansion observed in the first V-O shell (Table 1), which reaches 2.02 Å at $x = 5.0$, compared to the stoichiometric value of 1.93 Å, we estimate an increase in the lattice parameters of 5 - 10 %. This is significant because other transition metal oxide intercalation compounds, such as $Li_{1-x}CoO_2$, contract as Li is added, at least up to the stoichiometric composition of $x = 0$ in the case of $Li_{1-x}CoO_2$, due to partial screening of the oxygen-host ion Coulomb repulsion by Li^+ ions.[20]

3. Figs. 4 (a), (b), and (c) show that peaks corresponding to the second and third shells decrease dramatically in amplitude with in x values above 1.5, implying a decrease in local order beyond the first V-O octahedra. Fits for these more distant shells have much greater uncertainty and are k weighting dependent. Evidently, the increase in symmetry of the local octahedra is accompanied by increasing disorder at longer distances, which is not surprising as the lattice must distort to accommodate the changes in shape of the octahedra. This trend is summarized in Fig. 5(b), which plots the ratio of peak 1 to peak 2 in the RDF as a qualitative measure of the

disorder. Evidently the disorder begins to appear around $x = 1.0$ and increases most rapidly around $x = 2.0$.

Fig. 5 shows that the pre-edge peak, the first V-O peak in the RDF, and the ratio of peak 1 to peak 2 in the RDF all imply that there are three distinct structural regions as a function of Li concentration. The initial region, characterized by a slight decrease in the octahedral symmetry, occurs for $x < 1$. The "transition" region, characterized by an increase in octahedral symmetry and a decrease in disorder beyond the local octahedra, occurs for $x = 1$ to $x = 3$. Finally, a relatively constant region occurs for $x = 3$ to $x = 5$, with the $x = 6$ sample anomalous.

^{7}Li NMR Measurements

1. NMR Spectra

As shown in Fig. 6(a) and Fig. 7, for $x < 1.5$ lineshapes are mostly symmetric (especially above room temperature) and narrow (about 15 kHz at 23° C). These featureless NMR lineshapes reveal a very small distribution of Li environments which can be described in terms of a single dominant site, implying that the Li ions intercalate into the host V_6O_{13} with little variation in environment from site to site. Linewidths broaden only slightly with decreasing temperature, as shown in Fig. 6(a), indicating that over this temperature range (-150 to 200 °C), the Li environment is fairly rigid and Li^+ ions are relatively immobile in the vanadium oxide host lattice. Spectral peak positions, relative to aqueous LiCl solution, are plotted as a function of x in Fig. 7. For $x < 2$ the peak positions are shifted towards the diamagnetic side (low frequency) of the reference frequency. This means that the interaction between paramagnetic V^{+4} and the ^{7}Li is smaller than expected, which is most simply interpreted as meaning that, although there must be

significant amounts of V^{+4} present, the Li^+ ions are more likely to be associated with oxide phases richer in V^{+5} rather than V^{+4} or V^{+3} at these Li concentrations ($x < 1.5$).

We now consider the changes in ^{7}Li linewidths for $x > 1.5$, shown in Fig. 6(b) and Fig. 7. At these higher Li concentrations, lineshapes are broader and anisotropic, reflecting the pronounced influence of paramagnetic dipolar effects and chemical shift anisotropy. This implies that incorporation of more lithium into V_6O_{13} causes the formation of a variety of Li sites; they can no longer be characterized by a single environment. This is not surprising, since both previous x-ray diffraction studies of $Li_xV_6O_{13}$ [2] and the present EXAFS results indicate that the host structure changes dramatically with x. While for small x the dominant host phase isV_6O_{13}, with increasing Li content other phases form, and the NMR lineshapes must reflect their presence. The asymmetry of the responses is more apparent at lower temperature. In particular, there is a diamagnetically shifted response which appears as a shoulder at lower frequency in the low temperature spectra, as shown in Fig. 6(b). Large paramagnetic and homonuclear dipole-dipole interactions smooth out the asymmetric contributions to the lineshape which hinders resolution of the various lithium responses. Peak positions change discontinuously as the lithium content is increased. A large paramagnetic shift of about 50 ppm occurs abruptly as the lithium content is increased from $x = 1.5$ to $x = 2.0$ (Fig. 7). This is presumably due to the increased effect of V^{+4} on the ^{7}Li response. Peak positions remain paramagnetically shifted for larger x, indicating the strong influence of V^{+4} (and/or V^{+3}) species, even though the EPR measurements described above show that the actual V^{+4} concentration begins to decrease with with increasing x for $x > 2$.

2. Spin-Lattice Relaxation Time (T_1) Measurements

T_1 data are normally extracted from exponential recovery profiles. In the case of $Li_xV_6O_{13}$, the recovery profiles were not exponential and could be fit using a minimum of two different exponential terms. The distribution of Li sites can be interpreted in terms of at least two distinct kinds of Li sites with vastly different T_1 values. The dominant sites (populated by over 90 % of the Li ions) are characterized by a rapid recovery (T_1 = 50 - 150 ms), which is typically observed in diamagnetic solids for ^{7}Li relaxing via strong paramagnetic mechanisms. Interactions with V^{+4} (and/or V^{+3}) are implied by the rapid recoveries and confirms our EPR result that all samples contain moderate to large amounts of V^{+4}. In addition, a weaker signal, representing at most 10 % of Li ions in the sample, is characterized by a much longer recovery time (T_1 = 2 - 10 s). This contribution is probably due to the presence of an impurity such as LiOH. We focus this discussion on only the dominant Li sites.

The effect of V^{+4} on the relaxation behavior of ^{7}Li is quite evident in the ln(T_1) versus inverse temperature results of Fig. 8. It is evident that the relaxation time T_1 reaches a constant value at low temperature (to the right in the 1/T plot of Fig. 8). Such saturation means that the temperature is low enough that thermal effects, which must vary with temperature, have become negligible, and a non-thermal relaxation mechanism dominates the relaxation. This non-thermal mechanism must be the paramagnetic dipolar interaction between ^{7}Li and the unpaired electron associated with V^{+4} and V^{+3}. Note also that the relaxation times for x = 5.0 are smaller than those for x = 1.5, a point we return to below.

We did not observe a minimum in T_1 in this temperature range, above -150 to 200 °C, which implies that the onset of large scale Li^+ motion occurs above 200 °C. This is additional evidence for the presence of rigid lithium environments at the temperatures studied (< 200 °C).

The lineshape analysis described above suggests that Li^+ ions preferentially locate near V^{+5} ions for $x < 1.5$, a conclusion confirmed by the relationship between T_1 and Li content shown in Fig. 9, which plots T_1 vs. x at three different temperatures. At all temperatures there is a distinct maximum in T_1, which increases up to $x = 1.5$ and decreases thereafter. The increase in T_1 reflects the decreasing coupling between ^7Li and V^{+4} with increasing x from 0.5 to 1.5. Since the strength of the magnetic dipolar interaction varies as the inverse cube of the distance between two spins, this presumably means the average distance between Li and V^{+4} ions increases with x, although the concentration of V^{+4} is, simultaneously, increasing. This apparent paradox is resolved by our earlier observation that with increasing x in this range, there is a tendency for Li to reside inside oxide phases rich in V^{+5}.

The decrease in T_1 for $x > 1.5$ may have several causes. At low x, Li ions tend to locate near diamagnetic V^{+5} sites. As the number of V^{+5} sites decreases, the average distance between Li ions and V^{+4} decreases, strengthening the paramagnetic relaxation mechanism and decreasing the relaxation time T_1. At higher values of x (>2), even though the V^{+4} population is decreasing, the paramagnetic relaxation mechanism of those ^7Li nuclei still coupled to V^{+4} still dominates. At high Li concentration, the relaxation mechanism results from contributions by the homonuclear dipole-dipole interactions between ^7Li nuclei and paramagnetic interactions with V^{+4} and V^{+3}.

Conclusions

The combination of EPR and x-ray absorption spectroscopy of the V host and NMR of the Li intercalant has given a comprehensive view of the changes in the electronic properties and physical structure which occur on the incorporation of Li into V_6O_{13}. Electronically, EPR and NEXFAS both imply that intercalation proceeds as expected; the Li donates electrons to the host and causes the gradual reduction of V and the formation of increasing amounts of V^{+4} and, at higher Li concentration, V^{+3}.

Structurally, several different regimes may be distinguished. For $x < 1$, both tne near edge and the extended x-ray absorption features imply that there is a slight increase in the distortion of the oxygen octahedra surrounding the V with increasing x. In the regime from $x = 1$ to 3, on the other hand, there is a dramatic increase in the symmetry of these local octahedra. In the third regime, beyond $x = 3$, there is little change. At the same time, particularly in the second and third regimes the disorder beyond the local octahedra increases and the lattice expands slightly. These three regimes are also apparent in the ^{7}Li NMR results. At low Li concentrations of x, the narrow linewidths suggest that Li ions, for the most part, occupy a single site and the increase in relaxation time T_1 implies that the Li ions tend increasingly to favor locations near V^{+5} ions. At higher concentrations, Li ions occupy a variety of sites, the formation of which is no doubt fostered by the increasing disorder. Strong relaxation mechanisms occur as the lithium content increases due to paramagnetic interactions with both V^{+4} and V^{+3}.

Acknowledgements

This work was supported, in part, from grants provided by the U. S. Office of Naval Research and the U. S. Army Research Office.

References

1. D. W. Murphy, Solid State Ionics **18-19**, 847 (1986).
2. C. Lampe-Onnerud, J. O. Thomas, M. Hardgrave and S. Yde-Andersen, J. Electrochem. Soc., **142** 3628 (1995).
3. D. W. Murphy, P. A. Christian, F. J. DiSalvo, and J. N. Carides, J. Electrochem. Soc.**126**, 497 (1979).
4. K. West, B. Zachau-Christiansen, T. Jacobsen, and S. Atlung, J. Power Sources **14**, 235 (1985).
5. H. K. Park, K. Podolske, Z. Munshi, W. H. Smyrl, and B. B. Owens, J. Electrochem. Soc. **138**, 627 (1991).
6. C. Lampe-Onnerud, P. Nordblad and J. O. Thoams, Solid State Ionics, **81**, 189 (1995).
7. B. Pecquenard, D. Gourier and N. Baffier, Solid State Ionics **78**, 287 (1995).
8. J. M. Cocciantelli, K. S. Suh, J. Senegas, J. P Doumerc, J. L. Soubeyroux, M. Pouchard, and P. Haenmuller, J. Phys. Chem. Solids **53**, 51 (1992).
9. R. Tossici, R. Marassi, M. Berretoni, S. Stizza, and G. Pistoia, Solid State Ionics **57**, 227 (1992).
10. A. Abragam and B. Bleaney, *Electron Paramagnetic Resonance of Transition Ions* (Dover, New York, 1986).
11. R. Tossici, R. Marassi, M. Berretoni, S. Stizza, and G. Pistoia, Solid State Ionics **67**, 77 (1993).
12. J. Wong, F. W. Lytle, R. P. Messmer, and D. H. Mayolotte, Phys. Rev. B **30** 5596 (1984).
13. B. K. Agarwal, *X-ray Spectroscopy*, Second Edition (Springer, New York, 1991).
14. R. D. Leapman, L. A. Grunes, and P. L. Fejes: Phys. Rev. B **26**, 614 (1982).

15. B. Hedman, J.E. Penner-Hahn, and K.O. Hodgson: In *EXAFS and Near Edge Structure III*, ed. by K.O. Hodgson, B.Hedman, and J.E. Penner-Hahn, Springer Proc. Phys., Vol 2. (Springer, Berlin, Heidelberg, 1984) p.64.

16. E. A. Stern, M. Newville, B. Ravel, Y. Yacoby, and D. Haskel, Physica B **208** & **209**, 117 (1995). These programs are copyrighted and licensed by the University of Washington. Contact E. A. Stern for further information.

17. A. F. Wells, *Structural Inorganic Chemistry*, Fifth Edition, (Clarendon Press, Oxford 1984).

18. K.-A. Wilhelmi, K. Waltersson, and L. Kihlborg, Acta Chem. Scand. **25**, 2675 (1971).

19. J. J. Rehr, R. C. Albers, and S. I. Zabinsky, Phys. Rev. Lett. **69**, 3397 (1992), and *Ab intio Multiple-Scattering X-ray Absorption Fine Structure and X-ray Absorption Near Edge Structure Code*, Copyright 1992, 1993, FEFF Project, Department of Physics, FM-15 University of Washington, Seattle, WA 98195.

20. E. Plichta, S. Slane, M. Uchiyama, M. Salomon, D. Chua, W. B. Ebner, and H. W. Lin, J. Electrochem. Soc. **136**, 1865 (1986).

Figure Captions

Fig. 1. Electron paramagnetic resonance spectra of $Li_xV_6O_{13}$ for various Li concentrations x.

Fig. 2. (a) Near edge x-ray absorption spectrum of the V 1s edge of $Li_xV_6O_{13}$ for various x, and on an expanded scale, (b) the pre-edge peak, and (c) the "white line" region.

Fig. 3. Geometrical model of V_6O_{13} used in fitting. V ions in three inequivalent sites V1, V2, and V3 are located at the center of O octahedra joined at edges and corners. The uppermost layer of octahedra is shaded.

Fig. 4. (a) Fourier transform of the extended x-ray absorption fine structure (radial distribution function) above the V 1s edge of $Li_xV_6O_{13}$ for various x, and the transforms compared to result of fits as described in the text for (b) $x = 0.5$ and (c) $x = 5.0$.

Fig. 5. Different measures of the structural changes near the V ions in $Li_xV_6O_{13}$ as a function of x. (a) The pre-edge intensity decreases with, and the amplitude of the first V - O peak in the RDF increases with, the local octahedral symmetry of the V ions. (b) The ratio of the first to second peak in the RDF increases with disorder.

Fig. 6. Nuclear magnetic resonance (NMR) spectra of $Li_xV_6O_{13}$ as a function of temperature for $x = 1.5$ and 5.0.

Fig. 7. Room temperature NMR spectral features in $Li_xV_6O_{13}$ for various *x*. (a) Peak positions, relative to aqueous LiCl,. (b) Peak full width at half maximum.

Fig. 8. Spin lattice relaxation times T_1 measured by NMR in $Li_xV_6O_{13}$ for $x = 1.5$ and $x = 5.0$, versus inverse temperature. Note the low temperature plateaurs characteristic of paramagnetic relaxation.

Fig. 9. Spin lattice relaxation times T_1 measured by NMR in $Li_xV_6O_{13}$ for various x, at room temperature, -100 °C, and -150 °C.

Shell	X-ray Diffraction V_6O_{13} (Å)	EXAFS Fit V_6O_{13} (Å)	EXAFS Fit $Li_5V_6O_{13}$ (Å)
First (V - O)	1.93	1.93	2.02
Second (V - V)	2.73	2.76	2.89
Third (V - O)	3.33	3.49	----

Table 1. Average distance between V and its first three near neighbors in $Li_xV_6O_{13}$, as computed from x-ray diffraction measurements and by fitting EXAFS measurements, for $x = 0$ and 5.0.

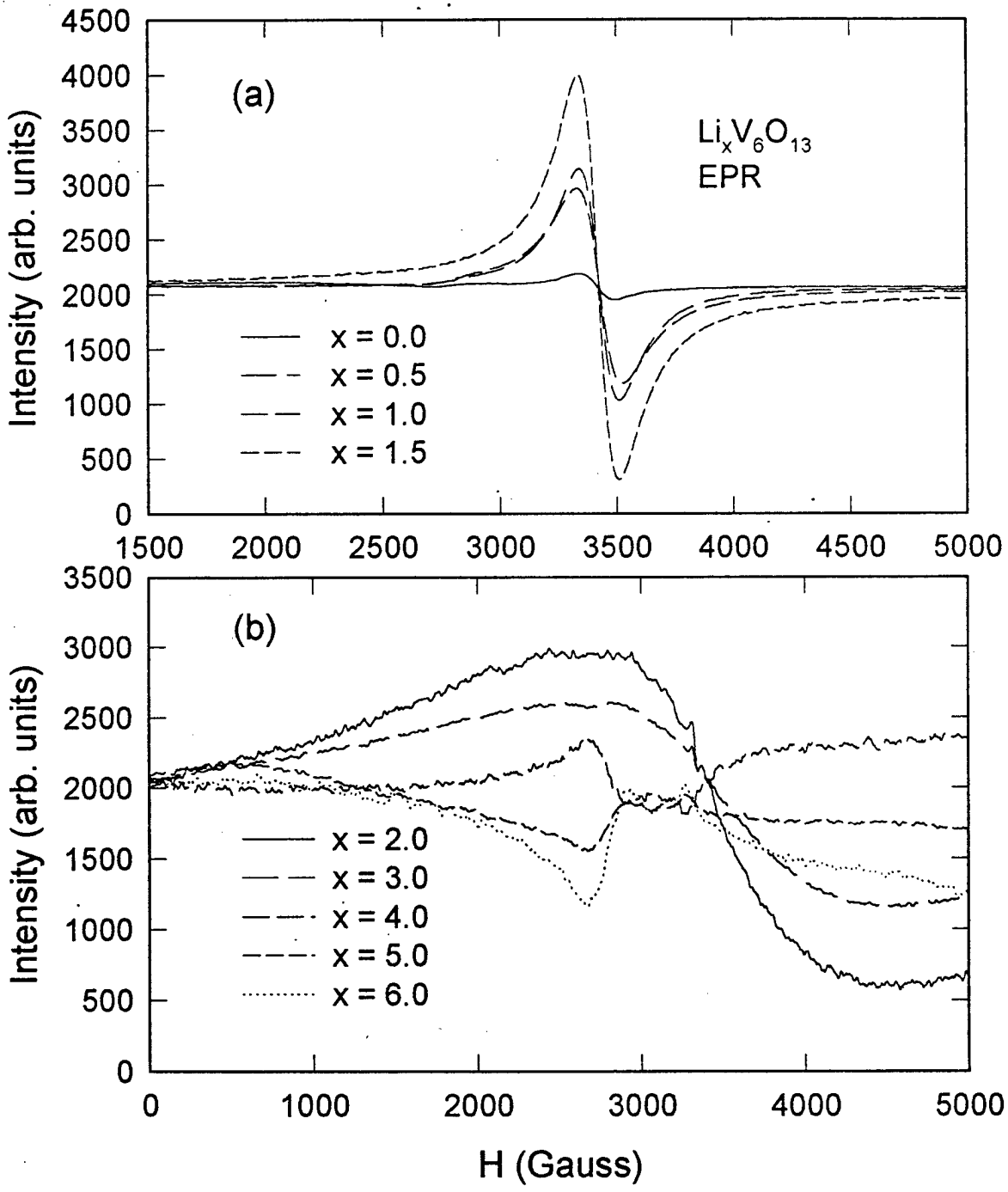

Fig. 1 Stalworth et al.

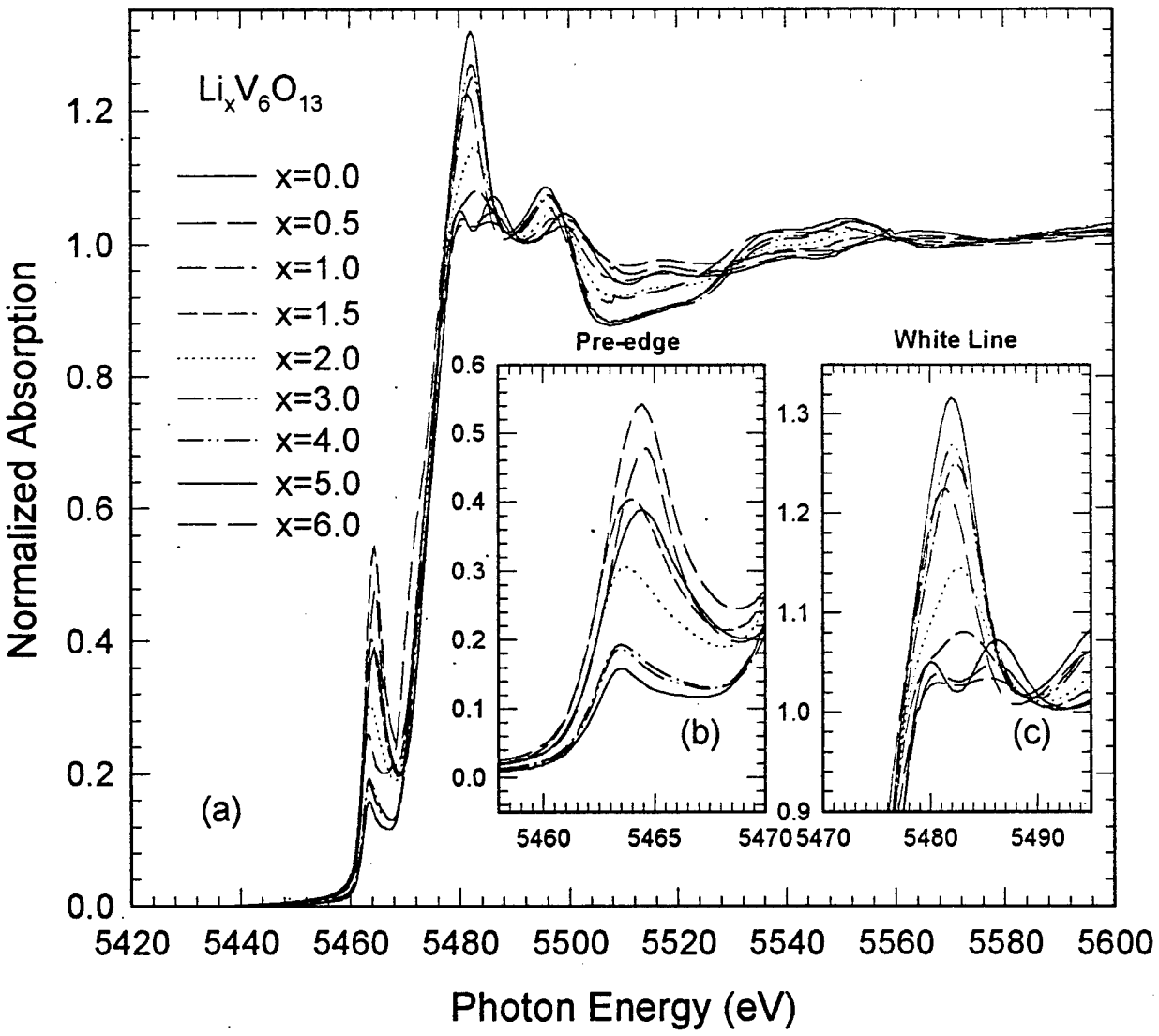

Fig. 2 Shellworth et al.

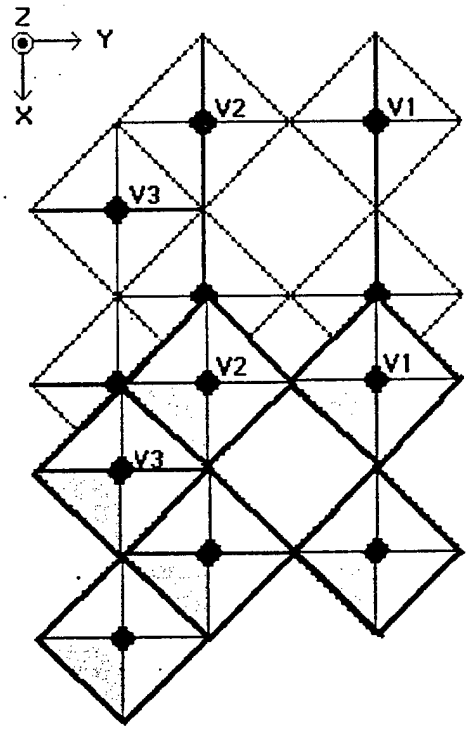

Fig. 3 Stallworth et al.

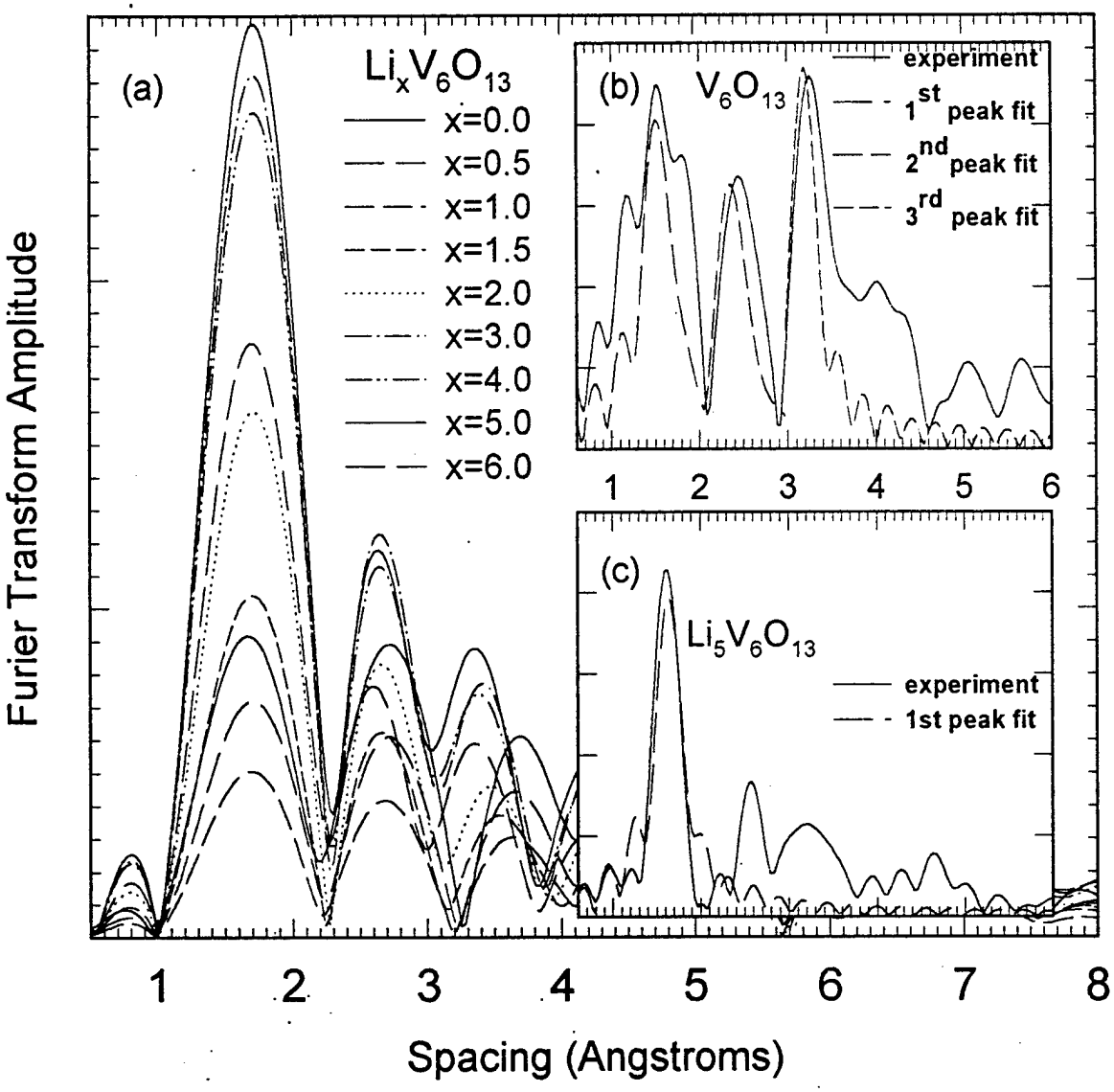

Fig. 4 Stallworth et al.

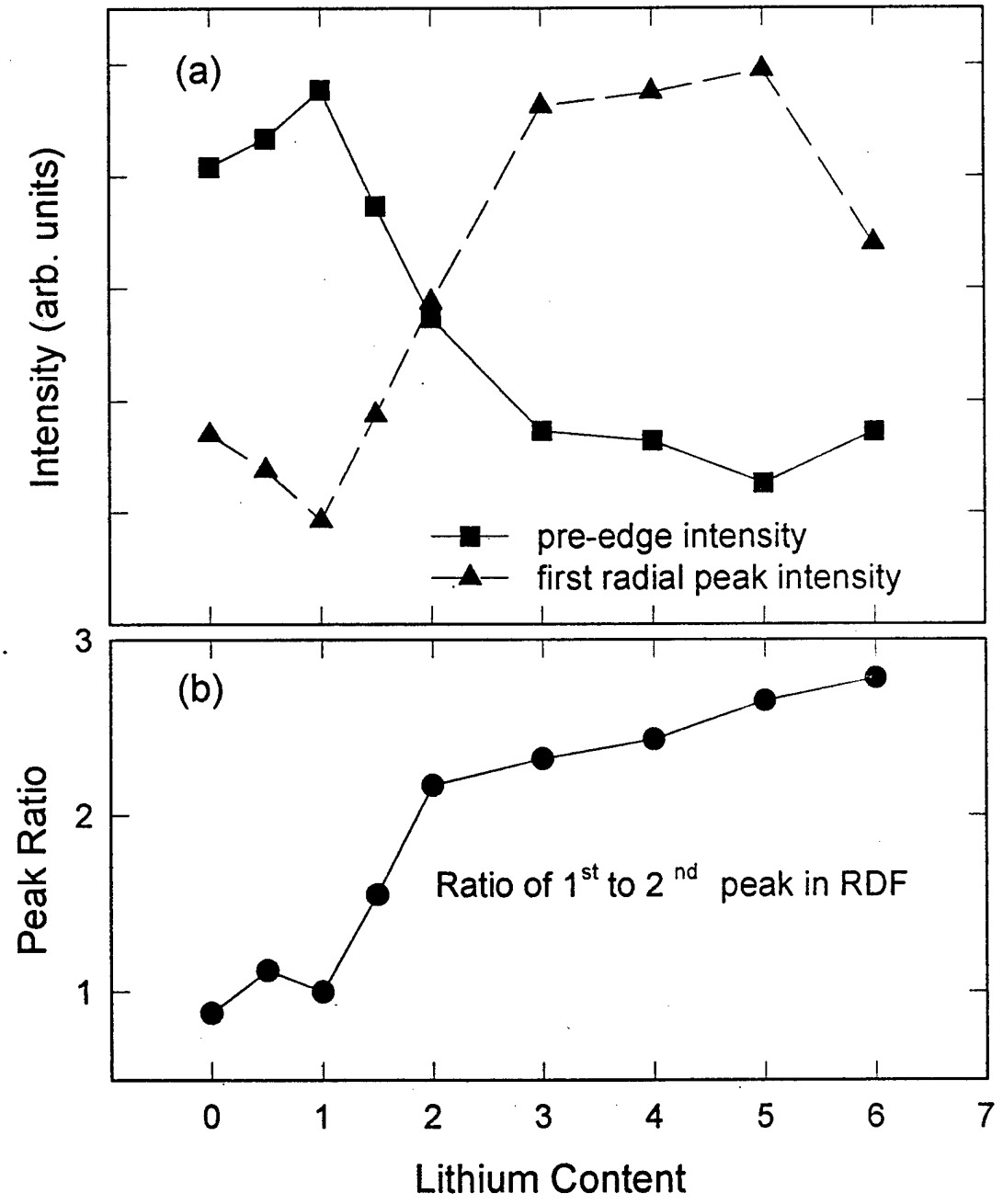

Fig. 5 Stallworth et al.

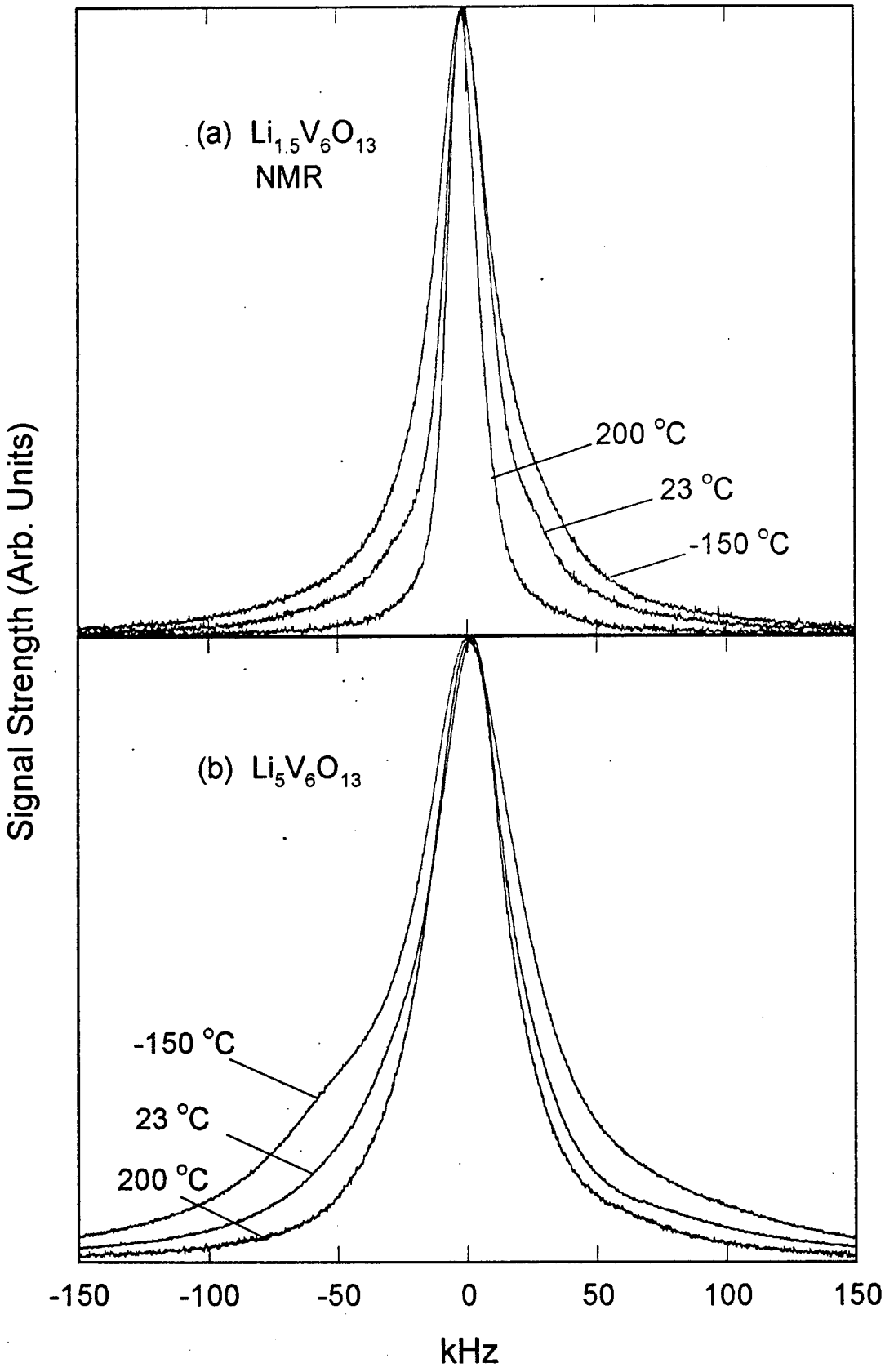
(a) $Li_{1.5}V_6O_{13}$
NMR
200 °C
23 °C
-150 °C
(b) $Li_5V_6O_{13}$
-150 °C
23 °C
200 °C
Signal Strength (Arb. Units)
-150
-100
-50
0
50
100
150
kHz

Fig. 6

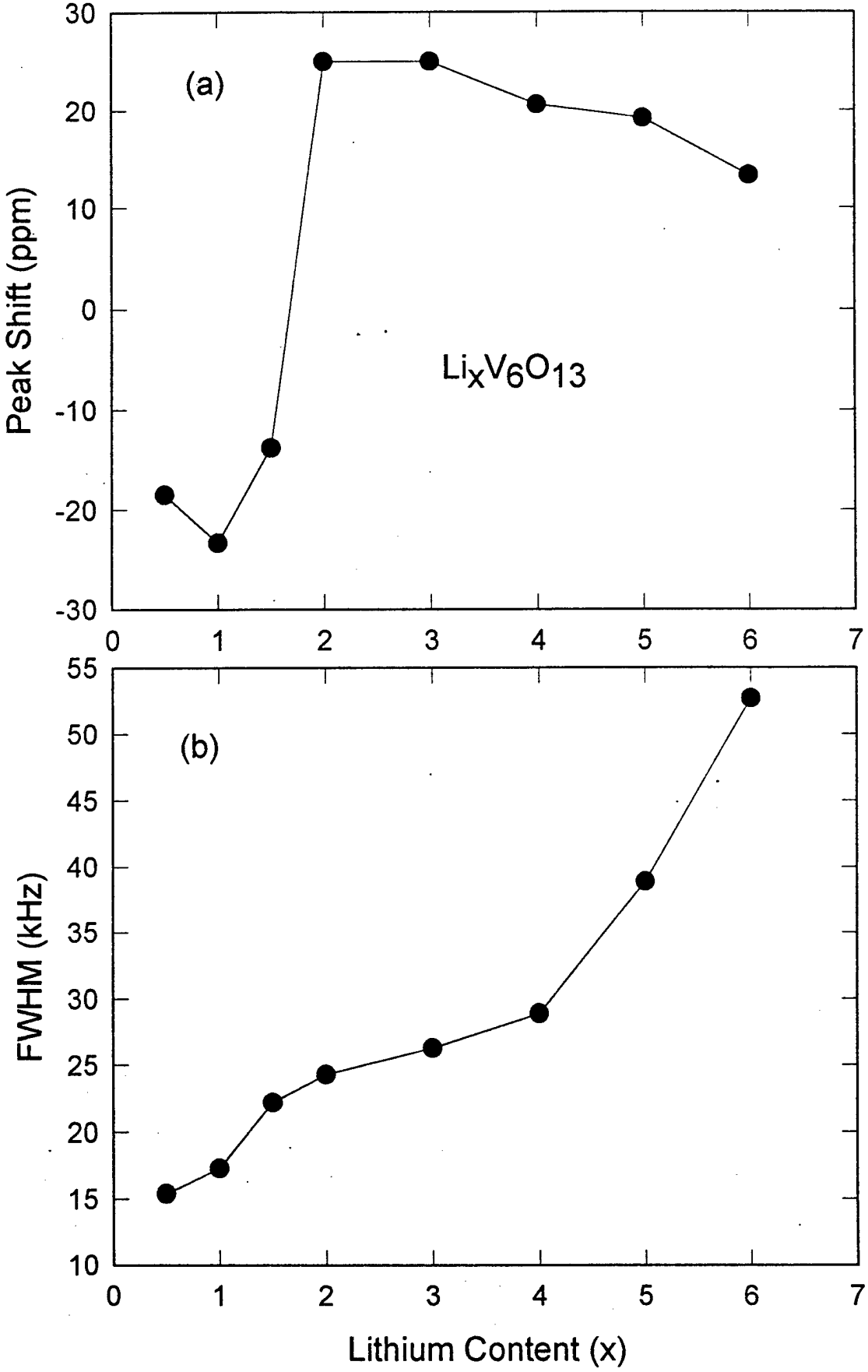
(a)
Peak Shift (ppm)
30
20
10
0
-10
-20
-30
$Li_xV_6O_{13}$
0
1
2
3
4
5
6
7
(b)
FWHM (kHz)
55
50
45
40
35
30
25
20
15
10
Lithium Content (x)

Fig. 7

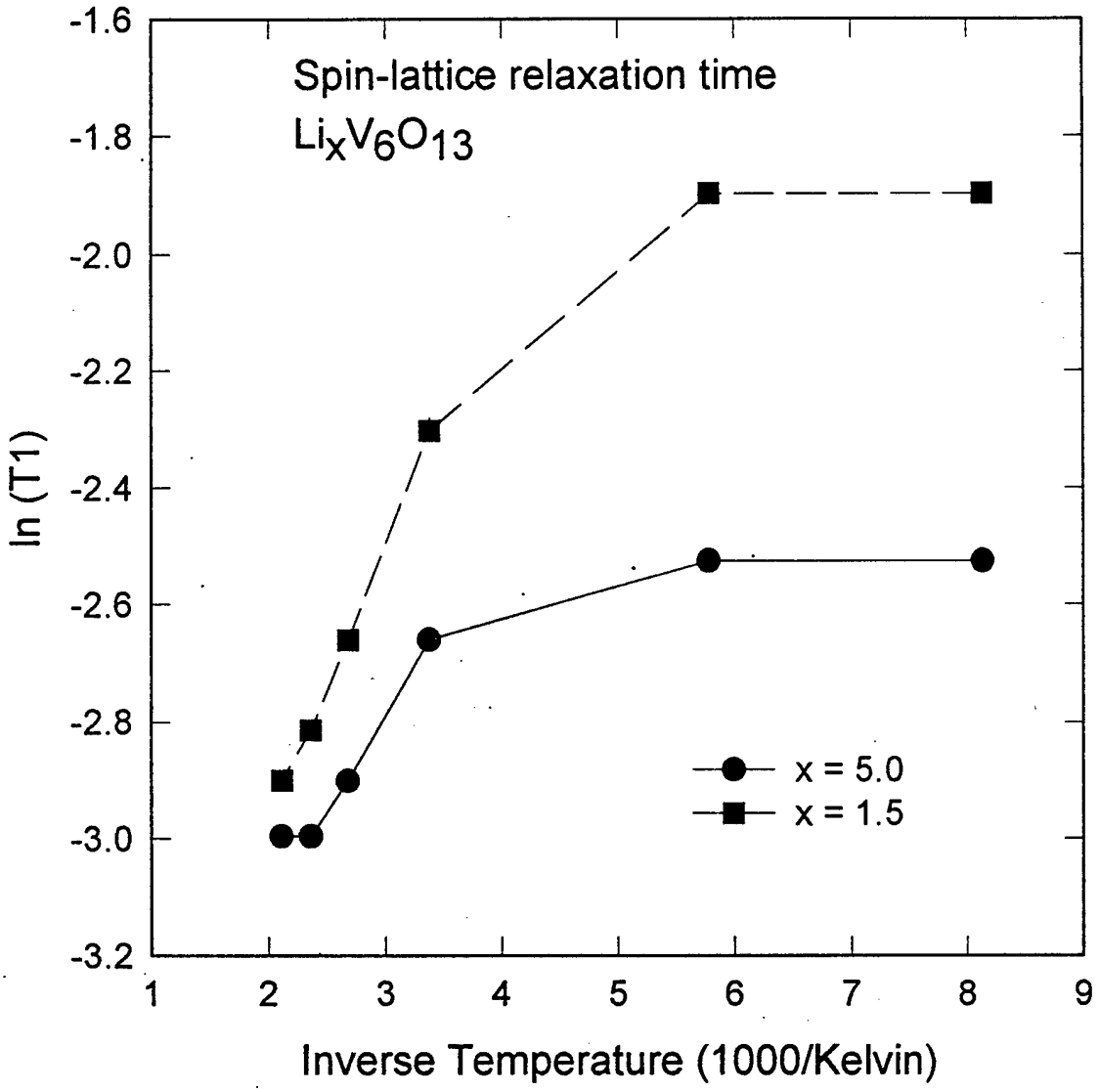

Fig. 8 Stallworth et al.

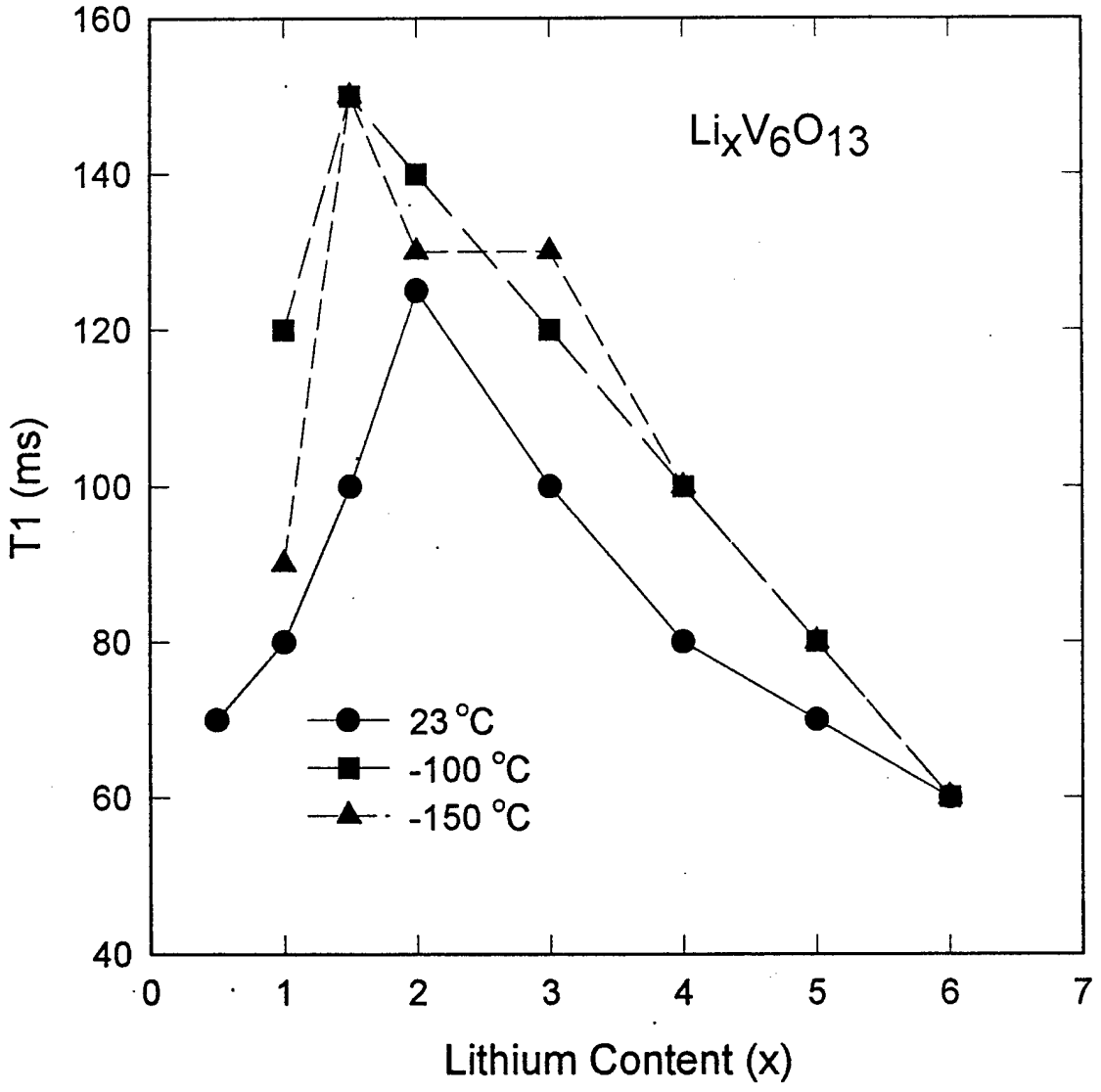

Fig 9 Stallworth et al.